On the correlation between radio and gamma ray luminosities of active galactic nuclei

A. Mücke[1]**, M. Pohl**[1]**, P. Reich**[2]**, W. Reich**[2]**, R. Schlickeiser**[2]**, C.E. Fichtel**[3]**, R.C. Hartman**[3]**, G. Kanbach**[1]**, D.A. Kniffen**[4]**,
H.A. Mayer-Hasselwander**[1]**, M. Merck**[1]**, P.F. Michelson**[5]**, C. von Montigny**[3,6]**, and T.D. Willis**[5]

[1] Max-Planck-Institut für Extraterrestrische Physik, Postfach 1603, D-85740 Garching, Germany
[2] Max-Planck-Institut für Radioastronomie, Postfach 2024, D-53020 Bonn, Germany
[3] NASA/Goddard Space Flight Center, Greenbelt, MD 20771, USA
[4] Hampden-Sydney College, P.O.Box 862, Hampden-Sydney, VA 23943, USA
[5] Hansen Experimental Physics Laboratory, Stanford University, Stanford, CA 94305, USA
[6] NAS/NRC Resident Research Associate

Abstract. The possibility of a correlation between the radio (cm)- and γ-ray luminosity of variable AGN seen by EGRET is investigated. We perform Monte-Carlo simulations of typical data sets and apply different correlation techniques (partial correlation analysis, χ^2-test applied on flux-flux relations) in view of a truncation bias caused by sensitivity limits of the surveys. For K-corrected flux densities, we find that with the least squares method only a linear correlation can be recovered. Partial correlation analysis on the other side provides a robust tool to detect correlations even in flux-limited samples if intrinsic scatter does not exceed ~ 40 % of the original γ-ray luminosity. However, if mean flux values of high variable sources are used we find the chance probability of high Spearman's correlation coefficient be significant underestimated. The analysis presented in this paper takes into account redshift bias and truncation effects simultaneously which was never considered in earlier papers.

Applying this analysis to simultaneously observed radio- and γ-ray data, no correlation is found. However, an artificial correlation appears when using the mean flux. This is probably due to the reduction of the dynamical range in the flux-flux relation. Furthermore, we show that comparing the emission in both spectral bands at a high activity state leads to no convincing correlation.

In conclusion, we cannot confirm a correlation between radio and γ-ray luminosities of AGN which is claimed in previous works.

Key words: galaxies: active – quasars: general – gamma rays: observations – methods: statistical

1. Introduction

Many attempts have been made in the past to investigate correlations between radio (cm)- and γ-ray luminosities of AGN (i.e. Stecker et al. 1993, Padovani et al. 1993, Salamon & Stecker 1994). By applying regression and correlation analysis to the 2.7 GHz- and 5 GHz-luminosity and the γ-ray emission in the EGRET energy band, a (nearly) linear correlation was found. The use of luminosities instead of fluxes, however, always introduces a redshift bias to the data, since luminosities are strongly correlated with redshift. Especially in samples which cover a wide range of distance, a correlation will appear in a luminosity plot even when there is no correlation in the corresponding flux densities (Elvis et al. 1978). Feigelson & Berg (1983) show that, if there is no intrinsic luminosity-luminosity correlation, no correlation will appear in the flux-flux relation even in flux-limited samples. On the other hand, intrinsic correlations between luminosities may be lost in the flux diagrams. The apparent correlation is maintained only when the underlying relationship is linear (Feigelson & Berg 1983). Furthermore, any observational uncertainties will hamper the finding of correlations using flux diagrams. It is therefore crucial to estimate the influence of the redshift bias on the correlations between the emission from the two wavebands. Non-parametric partial correlation coefficients (Kendall's τ or the Spearman rank correlation coefficient R_s) have been used to deal with this problem (Dondi & Ghisellini 1995). One limitation of these rank correlation tests is the failure to take into account possible changes in rank due to observational uncertainties. Observational flux-limits of the samples are another serious bias which influences any correlation analysis as they restrict the populated region in the luminosity-luminosity diagram to a narrow band. Therefore, Feigelson & Berg (1983) proposed to include all upper limits to avoid artificial correlations and incorrect conclusions (Schmitt 1985), and suggest the use of survival analysis. However, if the censored data points are

not distributed randomly, but localize a particular area, survival analysis may give misleading results (Isobe 1989). Furthermore, this analysis cannot account for a bias caused by misidentified sources or by objects which are completely lost due to the low sensitivity of the instrument. Those truncation effects must be seriously considered when EGRET data are used.

Another problem arises when considering the nature of the sources. Blazars are known to be strongly variable in the γ-ray as well as in the radio band on time scales of days to months (von Montigny et al. 1995). Therefore, simultaneous observations should be the adequate data for a correlation analysis. However, due to the lack of such data, the mean (Padovani et al. 1993, Setti & Woltjer 1994) or the brightest flux values (Dondi & Ghiselini 1995) of the sources have been used in the past. For highly variable sources this choice reduces the dynamical range in the luminosity-luminosity plot essentially, and can mimic a correlation.

In this paper, we evaluate the reliability of the partial correlation analysis in luminosity-luminosity plots as well as χ^2-fits in flux-flux diagrams for flux-limited truncated samples with strongly variable sources. For this purpose we perform Monte-Carlo simulations of typical data sets with known degrees of correlation and flux sensitivities, which is described in Sect. 2. No censored data are used. The simulations provide a useful test of how correlation analysis methods deal with such selection effects. The application of a database of EGRET-blazars in the radio (cm)- and γ-ray regime is presented in the last section.

Throughout this paper the Hubble constant $H_0 = 75$ km s^{-1} Mpc^{-1} and the deceleration parameter $q_0 = 0.5$ have been used.

2. Investigation of correlation techniques

2.1. Monte-Carlo simulations and correlation analysis

We consider a sample of objects with a wide range of distances observed in two spectral bands. To approximate the real case, we assume a sample of flat-spectrum radio quasars, with strong emission in the radio and γ-ray regime. We decide to use the '$\nu L(\nu)$' luminosity at the specific frequencies ν throughout this paper. The range of the local radio '$\nu L(\nu)$' luminosity L_R is chosen so that the simulated data resemble our database, and is set at $34 < \log L_R[\text{ erg s}^{-1}] < 50$. The lower limit of this interval is only important for data sets which are not affected by a sensitivity limit. The radio luminosity function ρ_{radio} which is assumed to be valid within the indicated luminosity interval is taken from Dunlop & Peacock (1990)

$$\rho_{radio} \sim [(\frac{L_R}{L_c(z)})^{0.83} + (\frac{L_R}{L_c(z)})^{1.96}]^{-1} \qquad (1)$$

where $L_c(z)$ is the 'evolving' break luminosity and was parametrized as $\log L_c(z) = 41.94 + 1.18z - 0.28z^2$ at 4.8 GHz and with the redshift z.

For the case of a $L_\gamma - L_R$ correlation the γ-ray luminosity is calculated from the relation

$$\log L_\gamma = A + B \log L_R + \epsilon(\sigma) \qquad (2)$$

where A and B are constants and free parameters. The term $\epsilon(\sigma)$ is a random noise component following a normal distribution with dispersion σ. We note that in this case the γ-ray luminosity distribution and evolution is proportional to the radio luminosity distribution and evolution.

If the radio and γ-ray luminosities are assumed to be un-correlated, the probability of detecting an object with a '$\nu L(\nu)$' luminosity L_γ in the γ-ray regime is calculated from the luminosity function ρ_γ of EGRET-blazars (Chiang et al. 1995)

$$\rho_\gamma \sim (\frac{L_\gamma}{L_B})^{-\gamma_2}\Theta(L_\gamma - L_B) + (\frac{L_\gamma}{L_B})^{-\gamma_1}\Theta(L_B - L_\gamma) \qquad (3)$$

where $\gamma_1 = 2.9$, $\gamma_2 = 2.6$, $L_B = 10^{46}\text{erg s}^{-1}h^{-2}$ and $h = H_0/100$ km s^{-1} Mpc^{-1}. A pure luminosity evolution is incorporated with $L_\gamma(z) \sim (1 + z)^{2.6}$ (see Chiang et al. 1995). The local '$\nu L(\nu)$' γ-ray luminosity range is again taken from the observation: $40 < \log L_\gamma[\text{ erg } s^{-1}] < 54$.

The objects are distributed in three dimensional space according to their evolution properties with redshifts z lying between $0.001 < z < 2.5$. The number of objects in each redshift bin dz has been independently determined by the differential redshift distribution $dN(z) = \psi_{radio}dV(z)$ expected from the radio luminosity function (with $dV(z)$ the comoving volume element and $\psi_{radio} = \int_{L_{lim}}^{\infty} \rho_{radio}dL$ the numerically integrated radio luminosity function). Using the relation

$$L_{band} = 7.6 \cdot 10^{57} S_{band} \cdot \bar{E}(1+z)^{\alpha-1}[(1+z) - \sqrt{1+z}]^2 \quad (4)$$

with S_{band} meaning either the radio flux S_{radio} or the γ-ray flux S_γ in erg cm^{-2} s^{-1} Hz^{-1}, $\bar{E}$ the mean photon energy in Hz and L_{band} the corresponding '$\nu L(\nu)$' luminosity in erg s^{-1}, we convert the luminosity to the flux. The term $(1+z)^{\alpha-1}$ is responsible for the K-correction. The average energy spectral indices for the respective spectral bands ($S_{band} \sim \nu^{-\alpha}$) are $\alpha_{radio} = 0$ for the radio band, and $\alpha_\gamma = 1$ for the γ-ray regime, where the latter also defines the mean photon energy of $\bar{E} = 470$ MeV. For the radio band we use 4.8 GHz photons. All objects which have fluxes lower than a specified limit are dropped from the data set. To account for the uneven exposure coverage of EGRET, we use a sigmoidal probability distribution for the detection of an object:

$$P(S_{lim}) = 1 - [1 + \exp{(C(S_{lim} + S_0))}]^{-1}$$

The parameters C and S_0 are chosen to be $C = 6.1(20.5)$ and $S_0 = -1.25(-0.55)$ for the radio (γ-ray) band. This means that the credibility limit in the radio band ranges from $\sim 0.5 \ldots 2$ Jy which can be considered as a result of an overlay of several radio catalogs with different credibility limits. The parameters corresponding to the γ-ray band are estimated from the flux threshold map of EGRET made from phase 1 and 2 of the mission. We created simulated data sets for different correlation slopes (B = 0.8, 1.0, 1.3 and 1.5), assuming either sensitivity limits as described above or perfectly sensitive detectors (i.e. flux densities down to 0.1 mJy in the radio band, and 10^{-11} photon s^{-1} cm^{-2} in the γ-ray regime are observed). For the simulations

of complete samples we assume the radio and γ-ray luminosity functions to extend down to luminosities below the original validity ranges. The simulations were done until each sample contains N = 25 and 12 objects which are typical numbers for the simultaneously observed data sets and the flaring state samples, respectively. For each parameter set the whole procedure was then repeated 100 times.

For generating data sets which consists of the mean flux value of the individual objects, the simulation procedure has to be modified. We derive the mean values for each source by averaging its historical minimum S_{min} and maximum S_{max}. In the radio band the activity distribution P(A) of EGRET sources has been determined based on 2.8cm-monitoring data obtained between 1991 to 1993 at the 100-m-Effelsberg Telescope (Mücke et al. 1996). As the relation

$$S_{radio} = S_{radio,min}(1 + \frac{\delta S}{S_{radio,min}}A)$$

applies with $\delta S = S_{radio,max} - S_{radio,min}$ the amplitude of the variability, we can compute the historical minimum and maximum, and therefore the mean flux value for each object. We take $\delta S = 2.1 S_{radio,min}$ which is the average variability of our 4.8 GHz data base consisting of > 100% variable sources. Again we omitted objects with a historical minimum flux lower than the credibility limit. In the γ-ray regime the activity distribution is not known. Therefore we determine the historical minimum and maximum by computing a γ-ray flux according the the γ-ray luminosity function for several times. This procedure simulates the average sampling of each source which is about three for our EGRET data. In order to account for our using > 100% variable sources we only accept those sampling sets which have historical maxima of at least two times the historical minimum in the case of all three observations lying above the sensitivity limit, or at least two times the sensitivity limit for one observation being below this limit. For the historical minimum we require that it must lie above the sensitivity limit.

We then analysed the data sets using Spearman's rank order partial correlation coefficient R_s (Macklin 1982). The partial correlation describes the relationship between two variables when the third variable is held constant. In this way the strong redshift dependence of the radio and γ-ray luminosity can be eliminated. To date the behaviour of Spearman's correlation coefficient in the presence of upper limits caused by sensitivity limits of the data sets is not known, in contrast to Kendall's τ, a further non-parametric correlation coefficient. The parametric methods are more efficient if one knows the exact distribution of the data. However, in astronomy we do not know the exact distribution functions and hence the non-parametric methods are usually preferable. There has also been some debate whether correlations can be discovered more secure by comparing fluxes instead of luminosities (Elvis et al. 1978). In order to examine how accurately flux-flux diagrams recover quantitative information from the data when flux-limits and uncertainties are taken into account, we carried out a χ^2-test of a linear relation $y = a + bx$ between the logarithms of the K-corrected flux densities. The flux density values were provided with uncertainties of 4% and 20% in the radio and γ-ray band,
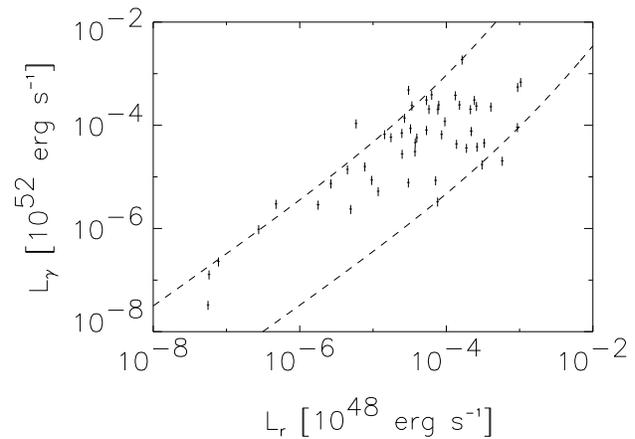

Fig. 1. Typical distribution of a **flux-limited** sample of objects which possesses **no correlation** between the radio and γ-ray luminosity. The dashed lines follow the sensitivity limits of the sample.
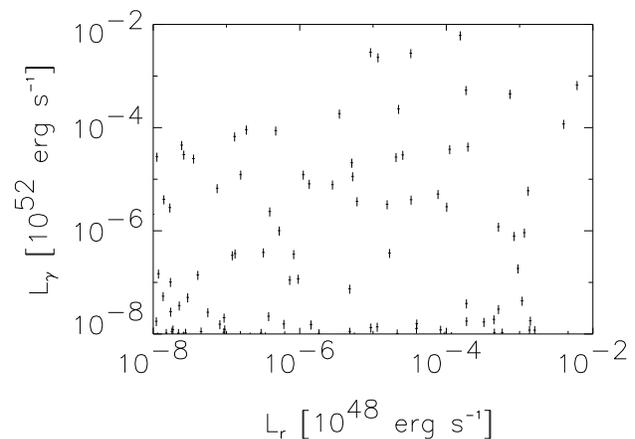

Fig. 2. Typical distribution of a **complete** sample of objects which possesses **no correlation** between the radio and γ-ray luminosity.

respectively, which are typical values for those spectral bands. The results are summarized in Table 1.

2.2. Results and discussion

The results of the partial correlation analysis (see Table 1) show that a correlation can be recovered at a significance level of > 99.5% for both complete and flux-limited samples provided that the intrinsic luminosity scatter is not too large ($\sigma \leq 0.05$). Increasing this noise factor up to $\sigma = 0.5$, a correlation can still be detected at a 90 % level. The most striking effect of a sensitivity limit is a generally lower correlation coefficient compared to complete data sets. High redshift objects can only be detected at high powers. Hence, sensitivity limits exclude mainly high-redshift objects with low luminosities. This effect is shown in Fig.1 and Fig.2 where simulated uncorrelated data are presented for a flux-limited and a complete sample of objects. While low-luminosity sources are rarely observed in flux-limited data sets, they are more common in samples which possess no flux-limits.

Table 1. Results of the correlation analysis of simulated data: partial correlation analysis using Spearman rank order correlation coefficient R_s (with the probabilities (*) of erroneously rejecting the null hypothesis (i.e. no correlation), and a least square analysis with the minimum χ^2, the goodness-of-fit probability (**) and the slope b of the fit as indicated above. The chance probabilities marked with an asterisk are derived from the simulated distribution of the correlation coefficients R_s. 100 trials were carried out with each sample containing N = 25 and 12 sources. For the mean values 600 test samples with N = 30 and 40 objects were generated. In case of a correlation, a random noise component with $\sigma = 0.05$ was chosen. The analysis were carried out between the logarithms of the luminosities and K-corrected flux densities, respectively. For the χ^2-fit, the flux density values were provided with uncertainties of 4% and 20% in the radio and γ-ray band, respectively. A correlation is said to exist for a chance probability (*) < 5 %, and a significance (**) > 50 % using the partial correlation analysis and least square method, respectively.

sample	N	R_s	probability*	corr. ?	χ^2_{min}	significance**	slope b	corr. ?
uncorrelated, flux-limited	25	0.061	0.461	NO	797.2	$1 \cdot 10^{-39}$	0.008 ± 0.036	NO
	12	0.053	0.508	NO	311.2	$2 \cdot 10^{-13}$	-0.015 ± 0.057	NO
uncorrelated, not flux-limited	25	0.024	0.492	NO	9721.3	0.	0.038 ± 0.011	NO
	12	0.057	0.517	NO	4126.0	0.	0.081 ± 0.017	NO
$L_\gamma \sim L_{radio}^{0.8}$, flux-limited	25	0.958	$1 \cdot 10^{-9}$	YES	63.6	0.077	0.741 ± 0.052	NO
	12	0.924	$2 \cdot 10^{-3}$	YES	26.9	0.170	0.746 ± 0.079	NO
$L_\gamma \sim L_{radio}^{0.8}$, not flux-limited	25	0.985	$6 \cdot 10^{-17}$	YES	55.4	0.038	0.824 ± 0.012	NO
	12	0.973	$3 \cdot 10^{-6}$	YES	22.1	0.146	0.824 ± 0.018	NO
$L_\gamma \sim L_{radio}$, flux-limited	25	0.967	$2 \cdot 10^{-11}$	YES	6.3	0.998	0.955 ± 0.058	YES
	12	0.940	$7 \cdot 10^{-4}$	YES	2.7	0.975	0.953 ± 0.085	YES
$L_\gamma \sim L_{radio}$, not flux-limited	25	0.987	$8 \cdot 10^{-18}$	YES	7.3	0.993	1.000 ± 0.013	YES
	12	0.974	$1 \cdot 10^{-5}$	YES	3.1	0.948	1.000 ± 0.021	YES
$L_\gamma \sim L_{radio}^{1.3}$, flux-limited	25	0.963	$6 \cdot 10^{-11}$	YES	78.3	$9 \cdot 10^{-3}$	1.164 ± 0.052	NO
	12	0.944	$2 \cdot 10^{-4}$	YES	33.0	0.056	1.183 ± 0.081	NO
$L_\gamma \sim L_{radio}^{1.3}$, not flux-limited	25	0.991	$1 \cdot 10^{-19}$	YES	122.2	0.0012	1.229 ± 0.012	NO
	12	0.981	$1 \cdot 10^{-6}$	YES	48.5	0.029	1.225 ± 0.019	NO
$L_\gamma \sim L_{radio}^{1.5}$, flux-limited	25	0.971	$4 \cdot 10^{-13}$	YES	276.6	$6 \cdot 10^{-8}$	1.076 ± 0.045	NO
	12	0.948	$2 \cdot 10^{-4}$	YES	104.3	$4 \cdot 10^{-3}$	1.107 ± 0.069	NO
$L_\gamma \sim L_{radio}^{1.5}$, not flux-limited	25	0.990	$1 \cdot 10^{-16}$	YES	467.7	$1 \cdot 10^{-22}$	1.322 ± 0.014	NO
	12	0.981	$2 \cdot 10^{-6}$	YES	195.7	$5 \cdot 10^{-5}$	1.334 ± 0.022	NO
mean, uncorr., flux-lim.	40	0.087	0.720*	NO	46.6	0.049	46.611 ± 46.637	NO
	30	0.074	0.819*	NO	31.4	0.060	31.383 ± 31.428	NO

This causes an overestimation of the redshift dependence in flux-limited samples. Therefore flux-limits seem to lower the degree of correlation.

Analysing flux-flux diagrams with the χ^2-tests of a linear relation can account for observational uncertainties in contrast to a partial correlation analysis. However, only a linear intrinsic correlation ($L_\gamma \sim L_{radio}$) can be recovered with this method no matter whether the sample obeys a sensitivity limit or not. Except for the case of a linear correlation the derived slopes of the correlations show misleading trends and the goodness of the χ^2-fit drops down when sensitivity limits restrict the flux range. The low range of apparent brightness, the 'distance random noise factor $D(z)^{2(B-1)}$,' (For $L_1 \sim L_2^B$ the corresponding fluxes S_1 and S_2 are related by $S_1 \sim S_2^B D(z)^{2(B-1)}$ with $D(z)$ the luminosity distance. For $B \neq 1$ each value S_2^B will be multiplied by a 'random' value $D(z)^{2(B-1)}$ (Feigelson & Berg 1983).), observational uncertainties and any intrinsic random noise factor $\epsilon(\sigma)$ cause a large scatter which prevents a reliable goodness-of-fit probability. In addition, we note that any intrinsic correlation $L_\gamma \sim L_R^B$ will be randomized by a factor $(1+z)^{\alpha_\gamma - 1 - B(\alpha_{radio} - 1)}$ ($\lesssim 3$ in our case) if the fluxes are not K-corrected. Especially for samples which cover a wide range of

redshifts but a small range of apparent brightness it is necessary to use K-corrected fluxes. Furthermore, when the intrinsic scatter causes a standard deviation from the expected luminosity of $\gtrsim 12\%$ ($\sigma > 0.05$), we even cannot find a linear correlation. Therefore, an intrinsic correlation could easily disappear using this method. In the case of a correlation with low intrinsic scatter ($\sigma \lesssim 0.05$), the right slopes are recovered within the parameter uncertainties in complete samples. Considering the correlation analysis of the mean flux values the situation changes in a interesting and surprising way. Though the partial correlation analysis of 600 flux-limited, uncorrelated test samples, each with 30 and 40 objects, gives on the average no positive signal, it turns out that the distribution of the correlation coefficients be not distributed like expected (Macklin 1982). Instead we find a significant higher probability of erroneously rejecting the null hypothesis (i.e. no correlation) in addition to an unexpected asymmetry of the R_s-distribution in the null hypothesis. To give some numbers we compare the correlation coefficient R_s and its chance probability derived from our observed data sets (see Table 2) with those derived from our simulation procedure. For $N = 28$ objects observed at 8 GHz the correlation coefficient $R_s = 0.405$ corresponds to a chance probability of $P = 0.035$

which can be compared with the numbers from the Monte-Carlo simulations: $P = 0.108$ for $R_s = 0.4$ corresponding to 40 cases of $R_s > 0.4$ out of 371 positive ones. This is a $> 6\sigma$ deviation from the expected chance probability. Enlarging the sample to 38 objects gives similar numbers (see Table 1). This can be explained as follows: Suppose, a number of variable objects with totally uncorrelated flux values are observed. The flux at the high activity states of the sources will be found at the upper right side of the correlation plot while the low activity states are crowded at the lower left side. After averaging the low and high activity data the resulting flux values occupy the narrow region in the middle of the correlation plot, and will arrange themselves along a straight line in the luminosity-luminosity-plot. This causes a bias which is not accounted for by the correlation methods. Hence, reducing the dynamical range in the flux-flux relation by the averaging procedure may cause an artificial correlation due to the underestimation of the erroneously rejected events.

3. Application to EGRET blazars

3.1. The sample

Our sample consists of 38 identified extragalactic point sources observed by EGRET between April 1991 to September 1993 (phase 1 + 2). EGRET covers the high energy γ-ray range from about 0.03 to 10 GeV with a field of view of about one-half steradian. The typical duration of an observation is two weeks. Only sources detected $< 25^o$ off-axis and with a significance $> 4\sigma$ at least once during the observation run are used in this analysis. The flux values used here are the integral flux (> 100 MeV), and are already published in Thompson et al. (1995).

Multifrequency radio observations of FSRQ with the 100-m-Effelsberg Telescope have been performed in parallel to the CGRO all-sky survey. All flat spectrum, variable sources stronger than 1 Jy at 5 GHz in the 50° field of view of EGRET have been observed quasi-simultaneously at 10.5 GHz, 5 GHz and 2.7 GHz. Sources, which have been detected by EGRET, were subsequently monitored at shorter time intervals. The observational method is described by Reich et al. (1993).

3.2. Data compilation

All sources used in this analysis are known to be variable. With a flux S and a redshift z, the 'νL_ν'-luminosity $\bar{L}$ is given by Eq. (4). For five objects with unknown redshift z, we set $z = 1$ which is the mean value of our sample.

In Fig. 3 the γ-ray flux is plotted against the simultaneously observed 2.7 GHz radio flux. The simultaneous observations were done at the Effelsberg telescope. We denote a pair of radio and γ-ray observations as 'simultaneous' if their observation dates do not differ by more than three weeks. Repeated EGRET observations of an AGN are taken as independent sources. The corresponding luminosity diagram is presented in Fig. 4.

We also investigated a possible correlation between the 8 GHz and the 4.8 GHz and the γ-ray luminosities in a flaring state. For the compilation of this data set, we have taken for
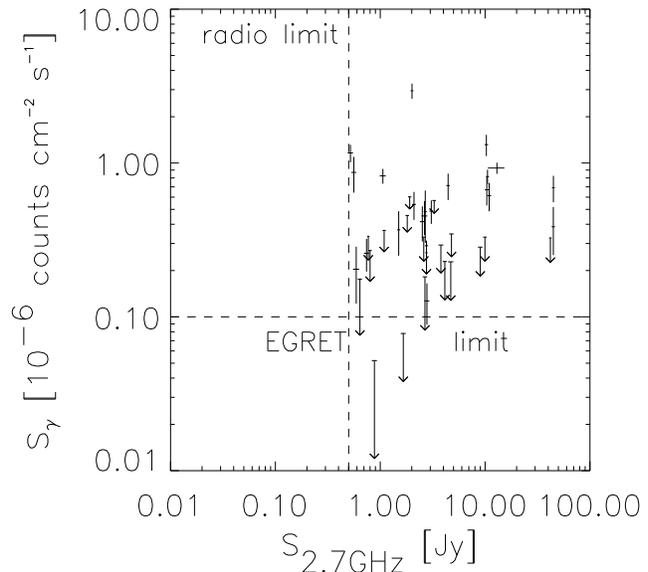

Fig. 3. Simultaneously observed γ-ray flux (> 100 MeV) (25 detections and 16 upper limits) versus 2.7 GHz-radio flux density. The dashed line follows the sensitivity limits of the sample.

each source the highest radio flux found in the literature (Aller et al. 1985, Kühr et al. 1981, White & Becker 1982, Wall & Peacock 1985, Reich et al. 1993, Fiedler et al. 1987, Seielstad et al. 1983, Waltman et al. 1991, Wright et al. 1990 and the PKSCAT90) and the maximal γ-ray flux observed by EGRET. In order to ensure that we really refer to the peak fluxes, we only use the historical flux values for > 100 % variable sources (= $(S_{max} - S_{min})/S_{min}$ with S_{min} the lowest detection or upper limit, and S_{max} the highest detection ever observed).

The average flux values at 4.8 GHz and 8 GHz were determined from the historical minimum and maximum found in the literature (reference see above). The mean γ-ray flux was calculated similarly from the minimum and maximum detection during phase 1 and 2 of the EGRET mission.

3.3. Results and discussion

The results of the correlation analysis between different kind of samples are presented in Table 2. We considered simultaneous detections (including upper limits UL) at 2.7 GHz and 10 GHz as well as data sets containing the respective highest flux of each source in the radio and γ-ray regime. To allow comparison to previous investigations, the average flux value of each source in the two spectral bands is also correlated. Analysing K-corrected flux-flux diagrams a positive signal could not be found for any of the considered samples. We therefore conclude that either an intrinsic scatter has smeared out a possible correlation or at least a linear correlation between the radio (cm)- and γ-ray emission does not exist.

In the last chapter we showed that for our typical data sets the Spearman's partial correlation coefficient can recover intrinsic correlations more secure compared to the χ^2-fit in flux diagrams

Table 2. Results of the correlation analysis of N observed data points: partial correlation analysis using the Spearman rank order coefficient R_s or Kendall's τ for the case of data sets where upper limits are included (with the probabilities (*) of erroneously rejecting the null hypothesis (i.e. no correlation)), and a least square analysis with the minimum χ^2, the goodness-of-fit probability (**) and the slope b of the fitted line. The chance probabilities marked with an asterisk are derived from Monte-Carlo simulations. The analysis were carried out between the logarithms of the luminosities and K-corrected flux densities, respectively.

| data	N	corr.coeff.	prob.*	corr. ?	χ^2_{min}	signif.**	slope b	corr. ?
10 GHz - γ-ray obs.(simult.det.)	25	0.158	0.465	NO	352.9	0.	-0.109 ± 0.029	NO
10 GHz - γ-ray obs.(simult.det.+UL)	42	0.079	0.288	NO	-	-	-	-
2.7 GHz - γ-ray obs.(simult.det.)	22	0.046	0.751	NO	298.5	0.	-0.031 ± 0.026	NO
2.7 GHz - γ-ray obs.(simult.det.+UL)	41	0.063	0.426	NO	-	-	-	-
max. 4.8 GHz - γ-ray obs.	12	0.594	0.053	marg.	225.9	$6 \cdot 10^{-43}$	0.450 ± 0.029	NO
max. 8 GHz - γ-ray obs.	11	0.363	0.314	NO	238.0	0.	0.477 ± 0.036	NO
4.8 GHz - γ-ray obs. (mean values)	38	0.347	0.114*	NO	159.3	$2 \cdot 10^{-17}$	-0.225 ± 0.041	NO
8 GHz - γ-ray obs. (mean values)	28	0.405	0.108*	NO	144.4	$2 \cdot 10^{-18}$	0.316 ± 0.073	NO
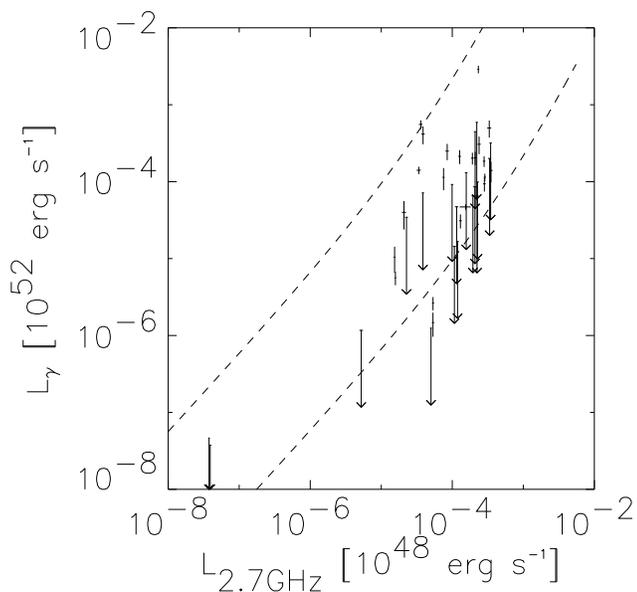
Fig. 4. Simultaneously observed γ-ray luminosity versus 2.7 GHz-radio luminosity. The dashed line follows the sensitivity limits of the sample.

using uncensored data. Nevertheless, even this method gives no significant indication for a correlation between simultaneous observations. This is also true when upper limits are taken into account and Kendall's partial correlation coefficient is used. For this method it is possible to state the significance level even for censored data (Akritas & Siebert 1996), in contrast to Spearman's R_s.

The marginal correlation found between the flaring 4.8 GHz- and γ-ray observations looses significance when considering the 8 GHz - γ-ray high-activity state relation which possess a high chance probability of $> 30\%$. The flaring state observations show only at one radio wavelength a marginal positive result, which we therefore consider as accidental. Hence, a convincing correlation between flaring detections does not exist.

Relating the mean 4.8 GHz- as well as the 8 GHz-radio and γ-ray luminosities gives a 2σ result for a positive correlation (see Table 2). However, using averaged flux values in highly variable sources induce a bias which could mimic a correlation. This effect is already discussed in Sect. 2.2.

Our results using Monte-Carlo simulations cannot confirm earlier findings concerning correlations between the radio (cm)- and γ-ray emission of blazars (Stecker et al. 1993, Padovani et al. 1993, Dondi & Ghisellini 1995, Salamon & Stecker 1994). Note, that the correlated quantities they used were not observed simultaneously although the sources are known to be highly variable. Instead, either the brightest (Dondi & Ghisellini 1995) or the mean fluxes (Stecker et al. 1993, Padovani et al. 1993) were taken. However, the use of average fluxes reduces the dynamical range in the flux diagrams and hence may mimic a correlation (see also Table 2). We conclude that our negative finding of a correlation between simultaneously observed sources is likely to be caused by the large scatter of the data points. Note also, that truncation effects as well as the influence of the redshift bias were not considered simultaneously in earlier works. Instead, mostly survival analysis was applied to eliminate biases caused by the sensitivity limits of the surveys. This method, however, was at then not able to also deal with a bias caused by the strong redshift-dependence of the correlated quantities. On the other hand, Dondi & Ghisellini (1995) have taken this effect into account by using partial correlation analysis, but neglected a bias caused by flux-limits. We therefore conclude that both, truncation effects as well as redshift bias, seriously influence the previously performed correlation analysis of radio- and γ-ray-loud blazars.

4. Conclusions

In previous work a correlation between the radio (cm)- and γ-ray luminosity of blazars seen by EGRET was claimed. For the correlation analysis biases caused by the limited sensitivity of the instruments and the strong redshift dependence of the luminosities must be considered. While the effects of flux-limits can be

taken into account by including upper limits, partial correlation analysis deals with the redshift bias. In this paper we considered both effects simultaneously in contrast to earlier works. For this purpose we performed Monte-Carlo simulations of a typical sample of variable blazars with known degree of correlation and completeness. We then analyzed the data sets by partial correlation analysis using the Spearman rank order correlation coefficient and a least square fit in flux-flux relations. The simulations reveal how correlation analysis deals with truncation biases caused by a limited sensitivity of the instrument. While in flux-flux diagrams only linear correlations can be recovered (provided that K-corrected fluxes are used) with the least square method, the partial correlation analysis gives correct results even for flux-limited sample. This is demonstrated for exponents $B = 0.8 \ldots 1.5$ ($L_\gamma \sim L_R^B$) with random noise factors up to an order of magnitude. Furthermore, in data sets with flux-limits, the partial correlation analysis gives a stronger redshift dependence of the luminosities compared to complete samples.

Applying the χ^2-method on flux-flux diagrams we found no evidence for a correlation between the simultaneously observed (2.7 GHz and 10 GHz) or flaring radio flux and luminosity (4.8 GHz and 8 GHz) and γ-ray luminosities above 100 MeV. The same result is obtained using the partial correlation analysis. The apparently positive signal between the average radio- and γ-ray luminosities is caused by the restriction of the dynamical range in the correlation diagrams.

We conclude that a simple power-law correlation between the radio (cm)- and γ-ray luminosities of AGN cannot be claimed.

Note however, that there is evidence that both radio- and γ-ray emissions from blazars are strongly beamed and not isotropic (von Montigny et al. 1995). The apparent source luminosity is related to the intrinsic luminosity by a factor which depends on the bulk Lorentz factor of the outmoving radiation source region within the jet and the angle between the line of sight and the jet axis. Those quantities are thought to be different for each object and each spectral band. Therefore, the beaming effect may smear out a possible correlation between the intrinsic luminosities, or worse, could cause a misleading correlation slope. Correlating luminosities which are corrected for beaming is unfortunately to date not possible since the Doppler factors in the γ-ray band are not known from observations.

The fact that we do not find any radio-γ-ray correlation for both simultaneously observed luminosities and high activity state observations has several important implications.

One may ask whether the lack of a correlation would rule out any of the proposed γ-ray emission processes in blazars. Especially the (inhomogeneous) synchrotron-self-Compton (SSC) models (Jones et al. 1974, Marscher 1980, Königl 1981, Marscher & Gear 1985, Ghisellini & Maraschi 1989, Marscher & Bloom 1992, Maraschi et al. 1992) seem to predict a correlation between the synchrotron emission and the inverse Compton component, as the optical synchrotron photons are upscattered to γ-ray energies by the same beamed relativistic electrons. After the source has undergone an internal evolution (cooling, ex-

pansion), its synchrotron photons can be observed in the radio regime. However, there are several reasons why we do not expect to find any relation between the luminosities in both spectral bands, even if we consider the SSC mechanism as the main γ-ray emission process. First, rapid variability, especially in the γ-ray regime, causes a large scatter in the luminosity and flux diagrams, and prevents recovering the true correlation slope even if a correlation would exist. Second, different relativistic Doppler factors D for the different objects induce an additional scatter since the observer considers different parts of the spectrum depending on the beaming factor D. Third, different γ-ray emission components may contribute differently for each individual object contaminating the relation with the radio band (i.e. the lack of strong emission lines in BL Lac objects indicates that the γ-ray emission induced by inverse Compton scattering of photons produced in the broad line region is small (Sikora et al. 1994). Note also, that the radio emission may be influenced by the contribution of a quiescent component (Valtaoja et al. 1988). Fourth, the different variability behaviour in the radio and γ-ray band points to a different spatial origin of the two luminosities which excludes a direct link. Fifth, there may be a time lag between the radio and γ-ray flare (Mücke et al. 1996, Valtaoja & Teräsranta 1995, Reich et al. 1993). Simultaneously observed luminosities are therefore not expected to obey a direct correlation. The same is true for the historical maximum relations between the radio and γ-ray regime since those flaring states must not be necessarily physically connected. Instead, the fluence of the two corresponding radio and γ-ray flares may be related. However, a single radio outburst can often not be isolated since radio flares often overlap especially at low cm-frequencies. Unfortunately, the lack of long-term γ-ray light curves of blazars does not enable a meaningful quantitative study at present. Last, the negative finding of a luminosity correlation could still be compatible with a similar energy content of the radio and γ-ray producing particles. Thus, we do not consider the non-correlation between simultaneously observed luminosities as strong evidence against the SSC model.

However, the non-correlation yields other astrophysical consequences. For both, the local luminosity density of blazars and their evolution properties, there is no hint for a direct link between radio (cm)- and γ-ray energies though the activity states may indicate a relation between the spectral bands (Mücke et al. 1996). So, the γ-ray luminosity function may not be reliably predicted from a known radio luminosity function and its evolution (Stecker et al. 1993, Salamon & Stecker 1994, Padovani et al. 1993, Erlykin & Wolfendale 1995, Dermer & Schlickeiser 1992, Stecker & Salamon 1996) or the extrapolation of a weak relation between mean fluxes to derive a Log N - Log S function for the γ-ray emission (Setti & Woltjer 1994). Instead, we suggest to model the γ-ray background induced by unresolved blazars by relating the energy content of particles to the γ-ray emission in AGN and take into account cosmological distances and the distribution of beaming angles, duty factors, etc.. This will be subject of future work.

This article was processed by the author using Springer-Verlag LaTeX A&A style file *L-AA* version 3.

References

Akritas, M.G., Siebert, J. 1996, MNRAS, 278, 919.

Aller, H.D., Aller, M.F., Latimer, G.E., et al. 1985, ApJS, 59, 513.

Chiang, J., Fichtel, C.E., von Montigny, C., Nolan, P.L., Petrosian, V. 1995, ApJ, 452, 156.

Dermer, C.D., Schlickeiser, R. 1992, Sci, 257, 1642.

Dixon, R.S. 1970, ApJS, 20, 1.

Dondi, L., Ghisellini, G. 1995, MNRAS, 273, 583.

Dunlop, J.S., Peacock, J.A. 1990, MNRAS, 247, 19.

Elvis, M., Maccacaro, T., Wilson, A.S., et al. 1978, MNRAS, 183, 129.

Erlykin, A.D., Wolfendale, A.W. 1995, J. Phys. G. 21, 1149.

Feigelson, E.D., Berg, C. 1983, ApJ, 269, 400.

Fiedler, R.L., Waltman, E.B., Spencer, J.H., et al. 1987, ApJS 65, 319.

Ghisellini, G., Maraschi, L. 1989, ApJ, 340, 181.

Gower, J.F.R., Scott, P.F., Wills, D. 1967, MNRAS, 71, 49.

Isobe, T. 1989, Thesis: Astronomical applications of survival analysis, Pennsylvania State University.

Jones, T.W., O'Dell, S.L., Stein, W.A. 1974, ApJ, 188, 353.

Königl, A. 1981, ApJ, 243, 700.

Kühr, H., Witzel, A., Pauliny-Toth, I.I., et al. 1981, A&AS, 45, 367.

Macklin, J.T. 1982, MNRAS, 199, 1119.

Maraschi, L., Ghisellini, G., Celotti, A. 1992, ApJ, 397, L5.

Marscher, A.P. 1980, ApJ, 235, 386.

Marscher, A.P., Gear, W.K. 1985, ApJ, 298, 114.

Marscher, A.P., Bloom, S.D. 1992, in: Proc. of the CGRO Science Workshop, NASA Conf. Pub. 3137, 346.

Mücke, A., Pohl, M., Reich, P., et al. 1996, Proc. 3rd Compton Symposium, A&AS submitted.

Padovani, P., Ghisellini, G., Fabian, A.C., Celloti, A. 1993, MNRAS, 260, L21.

PKSCAT90, Parkes Catalogue, 1990, Wright, A.E., Otrupcek, R.E. (eds.), Australia Telescope National Facility, CSIRO.

Reich, W., Steppe, H., Schlickeiser, R., et al. 1993, A&A, 273, 65

Salamon, M.H., Stecker, F.W. 1994, ApJ, 430, L21.

Schmitt, J.H.M.M. 1985, ApJ, 293, 178.

Setti, G., Woltjer, L. 1994, ApJS, 92, 629.

Sikora, M., Begelman, M.C., Rees, M.J. 1994, ApJ, 421, 153.

Seielstad, G.A., Pearson, T.J., Readhead, A.C.S., et al. 1983, Pub. Astr. Soc. Pac., 95, 842.

Stecker, F.W., Salamon, M.H., Malkan, M.A. 1993, ApJL, 410, L17.

Stecker, F.W. & Salamon, M.H. 1996, ApJ, in press.

Thompson, D.J., Bertsch, D.L., Dingus, B.L., et al. 1995, ApJS, 101, 259.

Valtaoja, E., Haarala, S., Lehto, H., et al. 1988, A&A, 203, 1.

Valtaoja, E., Teräsranta, H., 1995, A&A, 297, L13.

von Montigny, C., Bertsch, D.L., Chiang, J., et al. 1995, ApJ, 440, 525.

Wall, J.V., Peacock, J.A. 1985, MNRAS, 216, 173.

Waltman, E.B., Fiedler, R.L., Johnston, K.J., et al. 1991, ApJS 77, 379.

White, R.L., Becker, R.H. 1992, ApJS, 79, 331.

Wright, A.E., Wark, R.M., Troup, E., et al. 1990, Proc. Astron. Soc. Aust. 8, 261.